Liquid Crystals
Publication details, including instructions for authors and subscription information:
http://www.informaworld.com/smpp/title~content=t713926090

Thermotropic liquid crystals from *N*-alkylpyridinium halides ω-substituted with a mesogenic group

Dámaso Navarro-Rodriguez[ab]; Yves Frere[a]; Philippe Gramain[a]; Daniel Guillon[b]; Antoine Skoulios[b]
[a] Groupe de Chimie, Institut Charles Sadron, (CRM-EAHP) CNRS-ULP, Strasbourg Cedex, France [b] Groupe des Matériaux Organiques, Institut de Physique et Chimie des Matériaux de Strasbourg, (UMR-46) CNRS-ULP-EHICS, Strasbourg Cedex, France

To cite this Article Navarro-Rodriguez, Dámaso , Frere, Yves , Gramain, Philippe , Guillon, Daniel and Skoulios, Antoine(1991) 'Thermotropic liquid crystals from *N*-alkylpyridinium halides ω-substituted with a mesogenic group', Liquid Crystals, 9: 3, 321 — 335
To link to this Article: DOI: 10.1080/02678299108045568
URL: http://dx.doi.org/10.1080/02678299108045568

LIQUID CRYSTALS, 1991, VOL. 9, NO. 3, 321–335

Thermotropic liquid crystals from *N*-alkylpyridinium halides ω-substituted with a mesogenic group

by DÁMASO NAVARRO-RODRIGUEZ†‡, YVES FRERE†, PHILIPPE GRAMAIN†, DANIEL GUILLON‡, and ANTOINE SKOULIOS*‡

†Groupe de Chimie, Institut Charles Sadron, (CRM-EAHP) CNRS-ULP, 6, rue Boussingault, 67083 Strasbourg Cedex, France

‡Groupe des Matériaux Organiques, Institut de Physique et Chimie des Matériaux de Strasbourg, (UMR-46) CNRS-ULP-EHICS, 6, rue Boussingault, 67083 Strasbourg Cedex, France

(*Received 24 May 1990; accepted 28 October 1990*)

A series of *N*-alkylpyridinium halides ω-substituted with a 4-methoxybiphenylyloxy mesogenic group were synthesized and characterized. The molecules of these compounds contain three distinct parts: a flexible aliphatic chain, a rigid polarizable aromatic core, and a positively charged pyridinium ring associated with a negatively charged counterion. Their thermotropic liquid-crystalline behaviour was studied by differential scanning calorimetry and optical microscopy. Three types of smectic mesophase, namely A, B, and E, were identified by X-ray diffraction. Their structure consists of single layers of upright molecules laterally arranged head to tail. Segregated from the non-ionic parts of the molecules, the ionic end groups are set in double layers with the oppositely charged species facing each other and equally distributed between the two sub-layers. For the ordered smectic E phases, the anions are arranged in rows along the rectangular two dimensional unit cell diagonals with the pyridinium rings sandwiched between them in a chevron-type structure. As for smectic mesophases obtained with soaps, the smectic ordering described in the present work relies primarily on the electrical interactions of the ionic endgroups. Although present, the van der Waals repulsions of the aliphatic and aromatic moieties turn out to be ineffectual.

1. Introduction

Smectogenic molecules are generally formed of two distinct parts, fairly incompatible with one another. One regularly consists of flexible alkyl chains, the other is composed either of a polarizable, rigid and elongated aromatic core as in the vast majority of thermotropic liquid crystals [1], or else of a highly polar ionic group as, for instance, in the case of alkali metal soaps [2] or alkylpyridinium amphiphiles [3, 4]. The smectic ordering observed is then attributed to the amphiphilic character of the molecules, which is directly related to the effective repulsion of the molecular moieties and to their segregation in distinct layers periodically arranged in space [5].

We thought it of interest to investigate another class of more elaborate smectogenic materials, with three distinct parts in the molecules instead of only two. In that case, we would expect the constituent parts of the molecules either to combine their effective mutual repulsions, leading to systems with three distinct segregation microdomains periodically arranged in space, or else to have their mutual repulsions compensated in

*Author for correspondence.

0267-8292/91 $3·00

some way, leading to systems incompletely segregated. In this paper, we report the synthesis and the liquid-crystalline behaviour of a series of pyridinium halides obtained by quaternization of pyridine with halogenoalkanes of various lengths, ω-substituted with a 4,4′-methoxybiphenylyloxy group. In this series, the molecules are made of one alkyl chain carrying a pyridinium ring at one end and a non-ionic mesogenic group at the other. We also report results obtained with one similar compound, in which the alkyl spacer is replaced by a short polyethyleneoxide flexible chain.

2. Chemical synthesis

The quaternization of pyridine by alkyl halides is known to go faster the higher the dielectric constant of the solvent [6]. Among the variety of solvents liable to be used, pyridine itself seems most suitable: its dielectric constant is reasonably high ($\varepsilon = 12{\cdot}3$), and the quaternization reaction takes place in a homogeneous medium without side reactions similar to those that frequently occur in the presence of solvents such as methanol, nitrobenzene, and dimethylformamide; in addition, the reaction product readily precipitates. Using this process, a series of quaternary pyridinium salts were prepared by treating pyridine with ω-(4′-methoxy-4-biphenylyloxy)alkyl bromide and in one instance with 2-[2-[2-(4′methoxy-4-biphenylyloxy)ethoxy]ethoxy]ethyl bromide. The corresponding chloride and iodide derivatives were obtained from the bromide salts by reaction with an excess of silver chloride [7] or potassium iodide [8]. The chemical structures of the pyridinium compounds synthesized (designated in the following by C-n-X; X = Cl, Br, I; $n = 6$, 8, 10, 12; and for the oligoethyleneoxide derivative, by EtO-3-Br) are listed in table 1. Experimental details are given in §6.

The rather strong ionic interactions of these compounds are easily detected on a molecular level by ^{1}H NMR. This is shown by the important chemical shifts of the protons of the pyridinium ring and the methylene group directly attached to the nitrogen atom, which occur when the size of the anion changes; the smaller the anion the stronger the interactions. This is also shown by the chemical shifts of the water protons (1·7–1·8 ppm, in the hydrocarbon region) which take place when the pyridinium salts have been prepared or recrystallized in solvents containing traces of water; the water molecules incorporated in the crystals strongly interact with the methylene group next to the charged nitrogen. Elemental analysis shows that the degree of hydration depends on the nature of the counterion; chlorides crystallize with

Table 1. Chemical structure of the compounds studied.

Compound	Anion X^-	Spacer length	n
C-8-Cl	Cl^-	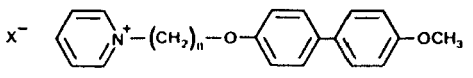	8
C-10-Cl	Cl^-		10
C-12-Cl	Cl^-		12
C-6-Br	Br^-		6
C-8-Br	Br^-		8
C-10-Br	Br^-		10
C-12-Br	Br^-		12
C-12-I	I^-		12
EtO-3-Br	Br^-		spacer $(CH_2CH_2O)_3$

one water molecule, bromides with one-half, and iodides with none. Products can, however, be easily obtained in an anhydrous form by heating in vacuum and then kept dry at ambient temperature.

3. Liquid-crystalline polymorphism

As shown by thermogravimetry, the compounds listed in table 1 were found to be thermally stable up to 180°C. Their polymorphic behaviour was studied by differential scanning calorimetry (Perkin–Elmer DSC 4, heating and cooling rates of 2·5°C/min), polarizing optical microscopy (Leitz Orthoplan, Mettler FP82 hot stage), and X-ray diffraction (Guinier focusing camera, bent quartz monochromator, $K_{\alpha 1}$ copper radiation from a Philips PW1009 X-ray generator, home made electrical oven). Typical

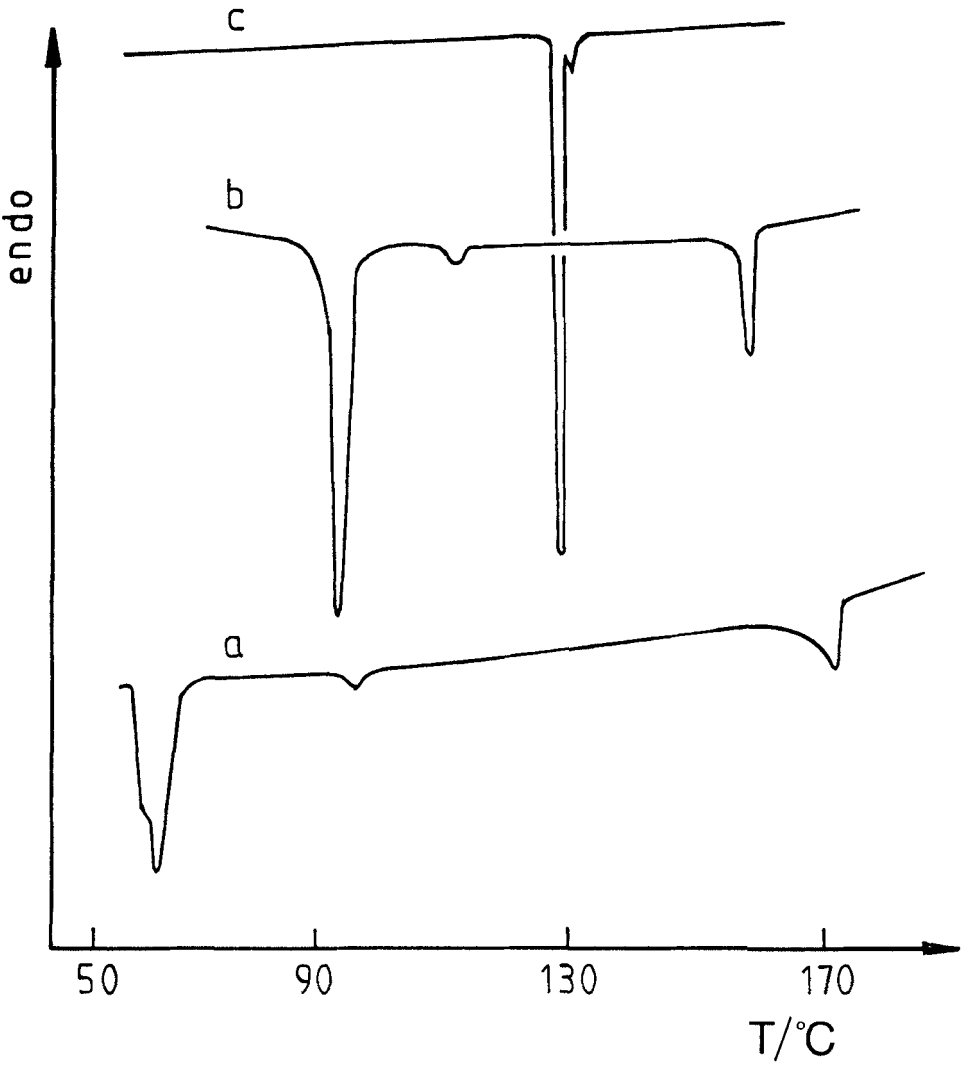

Figure 1. The DSC thermograms of (*a*) C-12-Cl, (*b*) C-12-Br, and (*c*) C-12-I, obtained upon cooling from the melt.

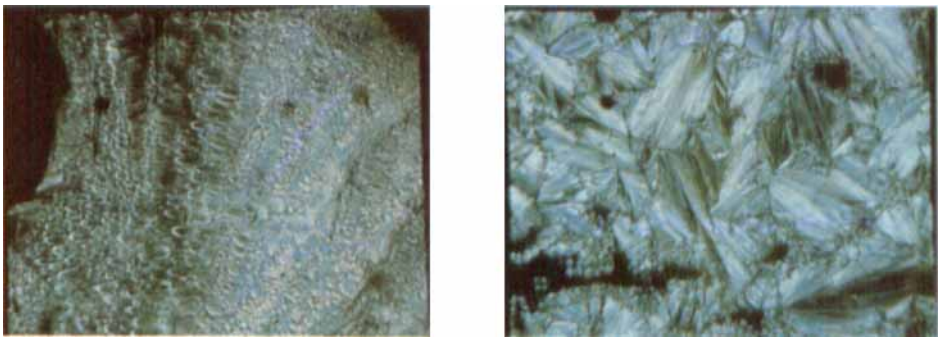

(*a*) (*b*)

Figure 2. The focal conic optical textures of C-12-Br in the smectic A phase obtained (*a*) by heating at 136°C from room temperature, and (*b*) by cooling at 153°C from the isotropic melt (crossed polars, magnification 180 ×).

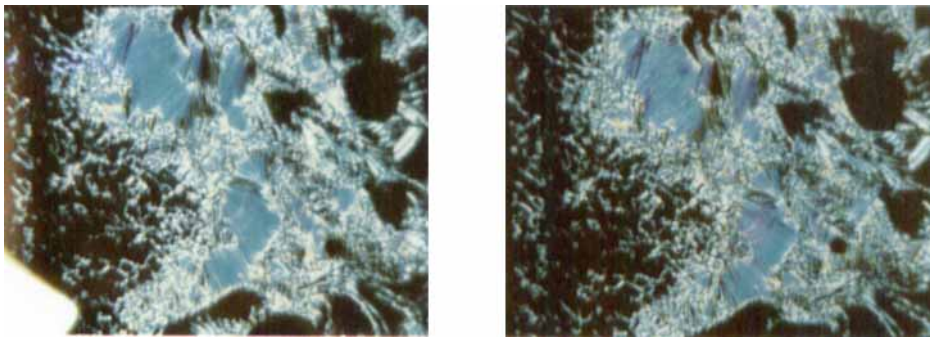

(*a*) (*b*)

Figure 3. The homeotropic and (striated) fan-shaped optical textures of C-10-Cl: (*a*) in the smectic A phase at 127°C, and (*b*) in the smectic B phase at 92°C, obtained by cooling from the isotropic melt (crossed polars, magnification 180 ×).

DSC thermograms and optical textures observed are shown in figures 1–3. The experimental observations are summarized in the polymorphic schemes:

C-8-Cl

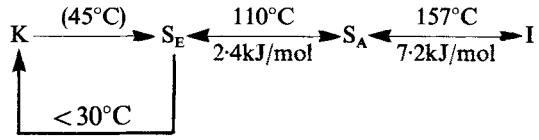

C-10-Cl

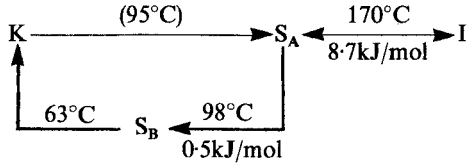

C-12-Cl

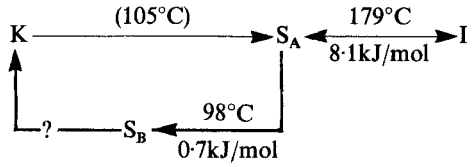

C-6-Br

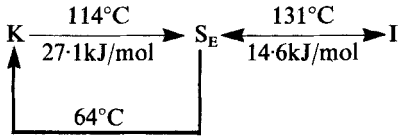

C-8Br

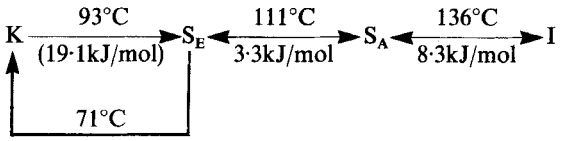

C-10-Br

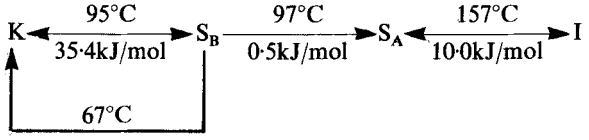

C-12-Br

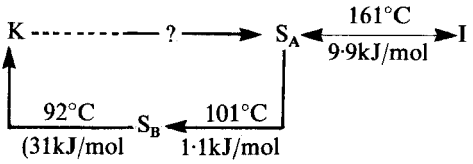

EtO-3-Br

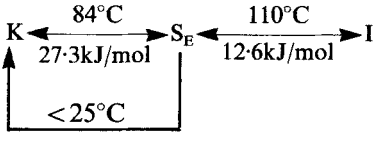

C-12-I

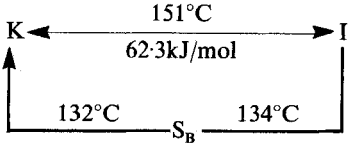

It is important to note that the transition from the liquid-crystalline to the crystalline state always shows a marked hysteresis upon cooling, simply related to the induction period of the crystallization process. In addition, the crystalline state presents a complex polymorphism, as for instance with C-12-Br, making it difficult to define clearly the melting transition into the liquid-crystalline state. Finally, in the special case of C-12-I, the smectic B phase was only observed upon cooling in a narrow range of temperature over very short periods of time.

4. Structure of the smectic masophases

X-ray diffraction was used to ascertain the nature of the various phases observed by DSC measurements and optical microscopy observations, and to determine their structural parameters. The crystalline nature of the phases at room temperature was demonstrated by the presence of many sharp Bragg reflections at both low and wide angles. The smectic nature of the liquid-crystalline phases at high temperature was characterized by the presence of two sharp equidistant reflections at low angles, related to the stacking period of the smectic layers. To analyse the structure, the stacking periods measured experimentally were compared with the calculated lengths of the molecules in their most extended configurations (see table 2). The lengths L were calculated by molecular modelling (Sybyl software from Tripos) with the counterions in the prolongation of the rod-like molecules. This immediately showed that, within the experimental accuracy, the smectic structures are all single layered, with the molecules oriented on average perpendicular to the smectic planes. No doubt, the molecules are laterally arranged head to tail as illustrated in figure 4. Such an arrangement is all the more plausible as it brings the anions close to the positively charged pyridinium rings and corroborates the usual up and down distribution of non-symmetrical molecules in liquid crystals. Similar structures with interdigitated molecules and anions sandwiched

Table 2. Layer spacings d_A, d_B, and d_E of smectic A, B, and E phases, measured at temperature T and compared with the molecular lengths L (the ionic diameters of Cl, Br, and I are of 3·62, 3·90, and 4·32 Å, respectively [9]).

Compound	L/Å	T/°C	d_A/Å	d_B/Å	d_E/Å
C-8-Cl	29·5	96	—	—	30·1
		140	31·1	—	—
C-10-Cl	32·0	90	—	32·0	—
		128	31·5	—	—
C-12-Cl	34·5	98	—	34·6	—
		135	35·0	—	—
C-6-Br	27·2	80	—	—	28·0
C-8Br	29·8	106	—	—	30·1
		135	29·6	—	—
C-10Br	32·8	80	—	32·0	—
		130	33·2	—	—
C-12-Br	34·8	107	—	35·8	—
		120	35·0	—	—
EtO-3-Br	31·3	80	—	—	30·7

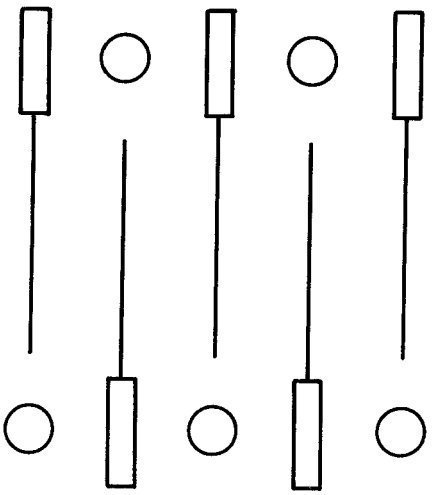

Figure 4. A schematic representation of the head-to-tail arrangement of the molecules within the smectic layers (circles denote the anions and rectangles stand for the pyridinium end groups).

between pyridinium rings have already been described in the literature, as for instance for smectic A 4-methyl-*N*-alkyl pyridinium halides [3] and *N*-methyl-4-alkylpyridinium iodides [4], as also for Langmuir–Blodgett films of *N*-docosylpyridinium tetracyanoquinodimethane doped with iodine [10].

The three different smectic phases identified by optical microscopy were definitely recognized and clearly distinguished from one another by the number and shape of the scattering signals in the wide angle region of the X-ray patterns. The smectic E phases were characterized by the presence of two rather sharp Bragg reflections around 4·5 and 4·1 Å, similar in every way to those generally observed with smectic E liquid crystals, as for instance with *p*-phenylbenzylidene-*p*-amino-*n*-pentyl cinnamate [11]. These reflections are indicative of a well-developed two dimensional ordering of the molecules within the smectic layers and can easily be indexed as d_{110} and d_{200} reflections from a two dimensional centred rectangular lattice. The rectangular cell parameters are shown in table 3 and compared to similar cell parameters found in the literature for other smectic E compounds. The molecular areas deduced from the cell parameters, $S = ab/2 \approx 22$ Å^2 (see table 3), agree with what is normally expected for the lateral packing area of rod-like smectogenic molecules [12]. They clearly indicate that, in these single layered smectic E phases, there are two molecules per unit cell, one at the centre, the other at the vertices.

Table 3. Wide angle Bragg reflections, d_{110} and d_{200}, and two dimensional rectangular lattice parameters of smectic E phases: *a* and *b*, lengths of unit cell sides; 2D, length of diagonal, ϕ, interdiagonal angle; *S*, molecular area.

Compound	d_{110}/Å	d_{200}/Å	*a*/Å	*b*/Å	*S*/Å^2	*D*/Å	ϕ/°
C-8-Cl	4·48	4·22	8·44	5·29	22·3	4·98	64
C-6-Br	4·55	4·03	8·06	5·51	22·2	4·88	69
C-8-Br	4·54	4·08	8·16	5·46	22·3	4·91	68
EtO-3-Br	4·54	3·95	7·90	5·55	21·9	4·83	70
PBAPC [11]	4·40	4·15	8·30	5·19	21·5	4·89	64
PM-2 [12]	4·54	4·01	8·02	5·51	22·1	4·87	69

As electrical interactions between molecules are known to be stronger than van der Waals interactions [13], a reasonable model for the spatial arrangement of the molecules in the smectic E phase under consideration must reasonably rely primarily on the arrangement of the ionic parts. Such a model is represented schematically in figure 5. It consists of layers of molecules with the ionic end groups facing each other in a way that could locally be taken as a double layer of oppositely charged ionic species. The anions are arranged in rows along the cell diagonals with the pyridinium rings sandwiched between them in a chevron-type structure; the crossing of the one

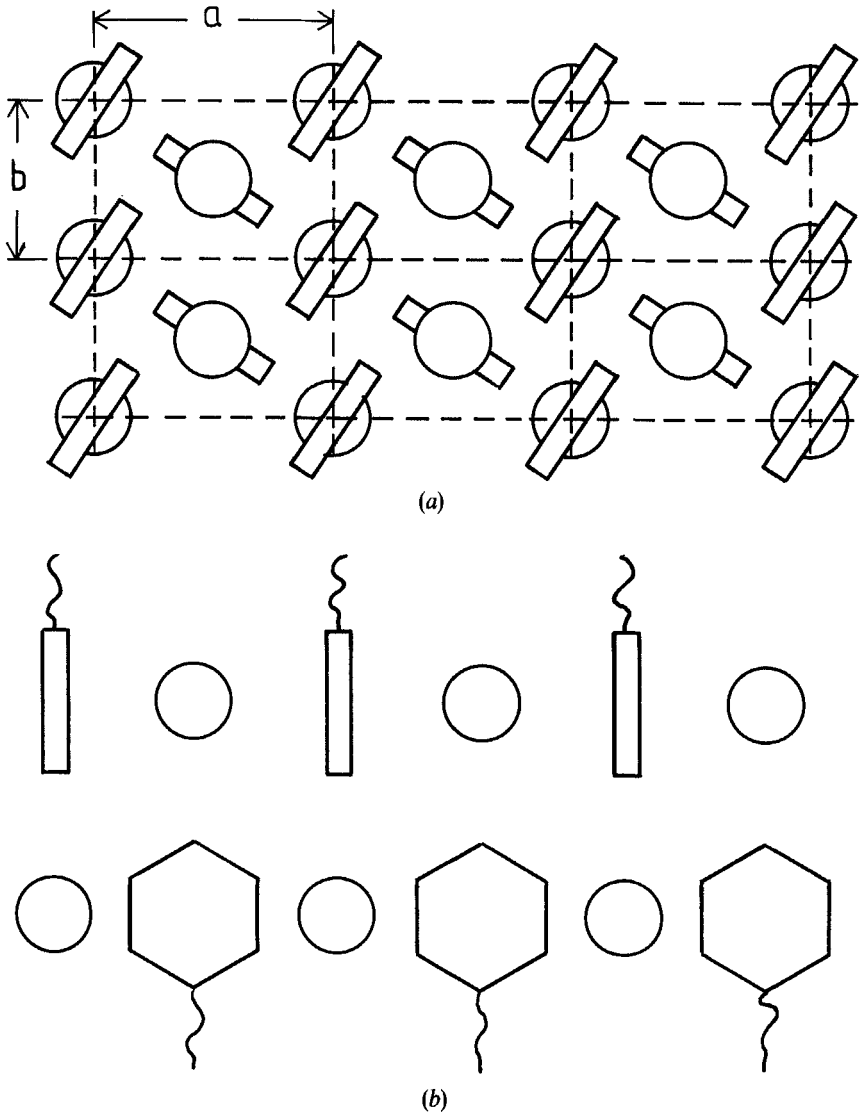

Figure 5. A schematic representation of the molecules in the smectic E layers: (*a*) top view of the projection of the molecular packing in one ionic sublayer onto the next: pyridinium rings represented by rectangles and anions by circles; (*b*) Side view of the arrangement of the pyridinium rings (rectangles or hexagons), anions (circles), and monionic moieties (wavy lines) along the cell diagonal.

dimensional rows of ions along the two diagonals ensures the rectangular symmetry of the two dimensional lattice. The anions are nearly in an axial position with respect to the pyridinium rings as needed from the standpoint of electrical interactions, the positive charge being delocalized over the pyridinium ring. As for the pyridinium rings, they are oriented nearly perpendicular to the $\langle 110 \rangle$ or $\langle 1\bar{1}0 \rangle$ diagonals of the rectangular lattice, depending upon whether they are located on the upper or the lower face of the ionic double layer (as defined in figure 7 (*c*), the angular deviation θ may be calculated to be about 11° from numerical values reported in table 3 for C-8-Cl and $e \approx 3{\cdot}6$ Å). In a given ionic sublayer, each ion is surrounded by four nearest neighbouring counterions at a distance D, and is in contact with one other counterion in the opposite sublayer. The resulting alternating distribution of ions is quite satisfactory from the standpoint of electrical interactions.

It is of interest to compare this ionic structure to that determined earlier by X-ray crystallography for *N-n*-butylpyridinium chloride in the crystalline state [14]. As shown in figure 6, the ionic species of this latter pyridinium salt are arranged rather uniformly, interacting with one another in all three dimensions of space. In spite of a tendency to aggregate, the butyl side chains are small enough just to fit in among the ions without perturbing significantly the somehow isotropic spatial distribution of the ions. It is clear, however, that in pyridinium salts with long alkyl side chains, as those studied here, a uniform distribution of the ions is no longer easy to achieve, and layered structures are obtained instead, with the ionic species interacting strongly in only two dimensions.

Although plausible as far as the electrical interactions are concerned, the structural model of the ionic double layer sketched in figure 5 has to be tested also with regard to the space filling requirements of the molecular packing. For this to be done, the structure was investigated by molecular modelling (Sybyl software from Tripos). As shown in figure 7 for the special case of C-8-Cl, the molecular packings found are entirely convincing, as they are close to ideal packings, that is to packings in which no molecules are suspended in empty space and none overlap [15]. Using the cell parameters given by X-ray diffraction (see table 3), the pyridinium rings and the counterions are indeed all in contact with one another as required.

In order to describe fully the structure, we must further specify the spatial arrangement of the non-ionic moieties of the molecules. These are attached to the nitrogen atoms of the pyridinium rings and point alternately up and down, outwards from the ionic double layers taken as the central part of the smectic layers (see figure 5 (*b*)). In agreement with the requirements of a single layered smectic structure and a molecular area per pyridinium ring of $ab \approx 44$ Å^2, the non-ionic moieties are interdigitated with those belonging to the adjacent smectic layers. Their molecular area, $S = ab/2$, is thus about 22 Å^2 (see table 3), as is usual for rod-like molecules in a smectic liquid crystal.

At this point, it is of interest to discuss the relative lateral position of the biphenyl groups in the non-ionic sublayers. It is clear that their lateral register is not as good as expected from the standpoint of their amphiphilic character [5]. This descrepancy is only apparent of course; it simply means that, in the interplay of the mutual effective repulsions of the ionic moities, the biphenyl groups and the alkyl chains, the repulsions leading to the segregation of the ionic species in preference to that of the methoxybiphenyl groups are more efficient. However, the lateral register of the biphenyl groups is not totally absent in all cases; for short alkyl chains for instance (see figure 8), the biphenyl groups overlap one another over about half their length. This partial overlap

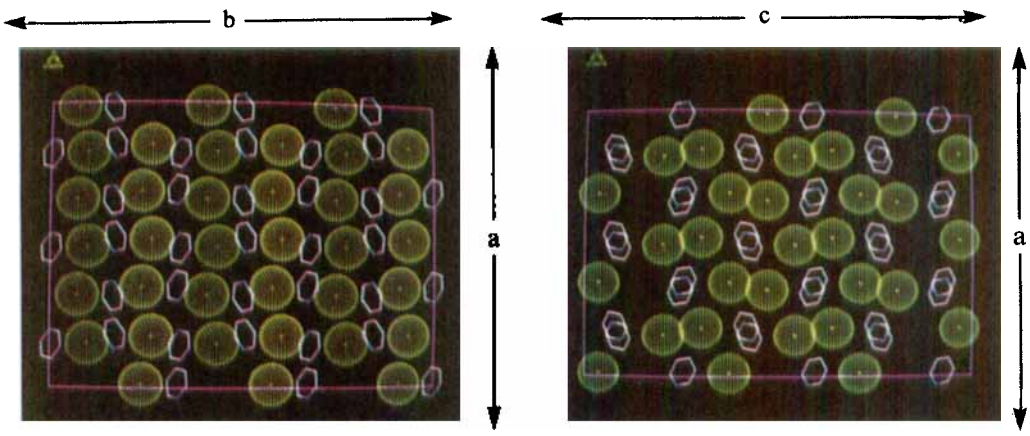

(*a*) (*b*)

Figure 6. The three dimensional arrangement of the pyridinium rings and chlorine anions (butyl chains and hydrogen atoms have been omitted for the sake of clarity) in the orthorhombic crystalline structure of *N*-*n*-butylpyridinium chloride, as obtained from the known atomic coordinates [14] by molecular modelling (Sybyl software from Tripos): (*a*) *ab*-projection, (*b*) *ac*-projection.

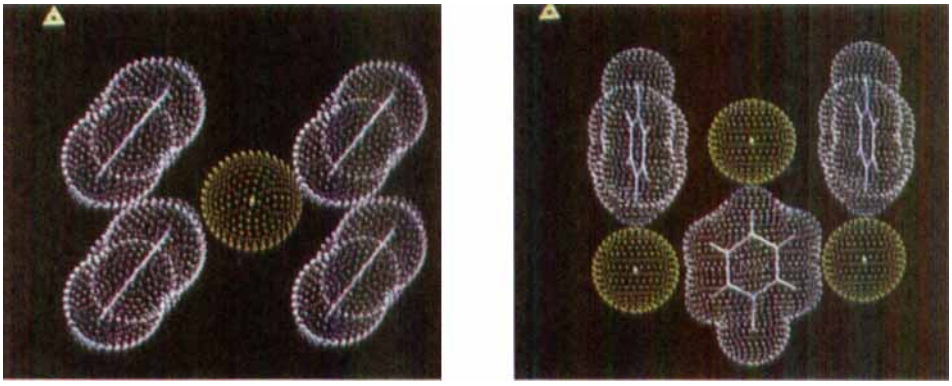

(*a*) (*b*)

Figure 7. Packingof the ionic species in C-8-Cl, as obtained by molecular modelling (Sybyl software from Tripos; intermolecular van der Waals radius of aromatic carbon atoms: 1·80 Å [15]): (*a*) top view of a single ionic sublayer; (*b*) side view of a double ionic layer along the cell diagonal; (*c*) schematic top view of the close packing of pyridinium rings (round-cornered rectangles) and anions (circles): $b\cos(\alpha)=e$; $\hat{n}$ is the normal direction to the pyridinium rings; $\hat{n}$ is tilted with respect to the rectangular cell diagonal by an angle $\theta=(\pi-\phi)/2-\alpha$.

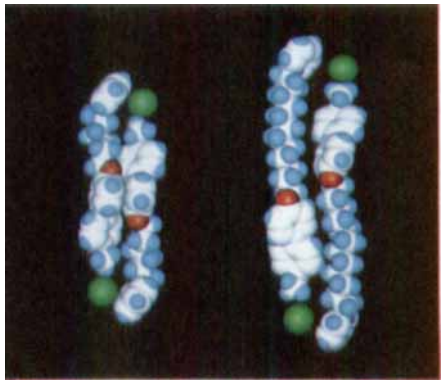

Figure 8. The head-to-tail arrangement of two C-6-Br and two C-12-Br molecules as obtained by molecular modelling.

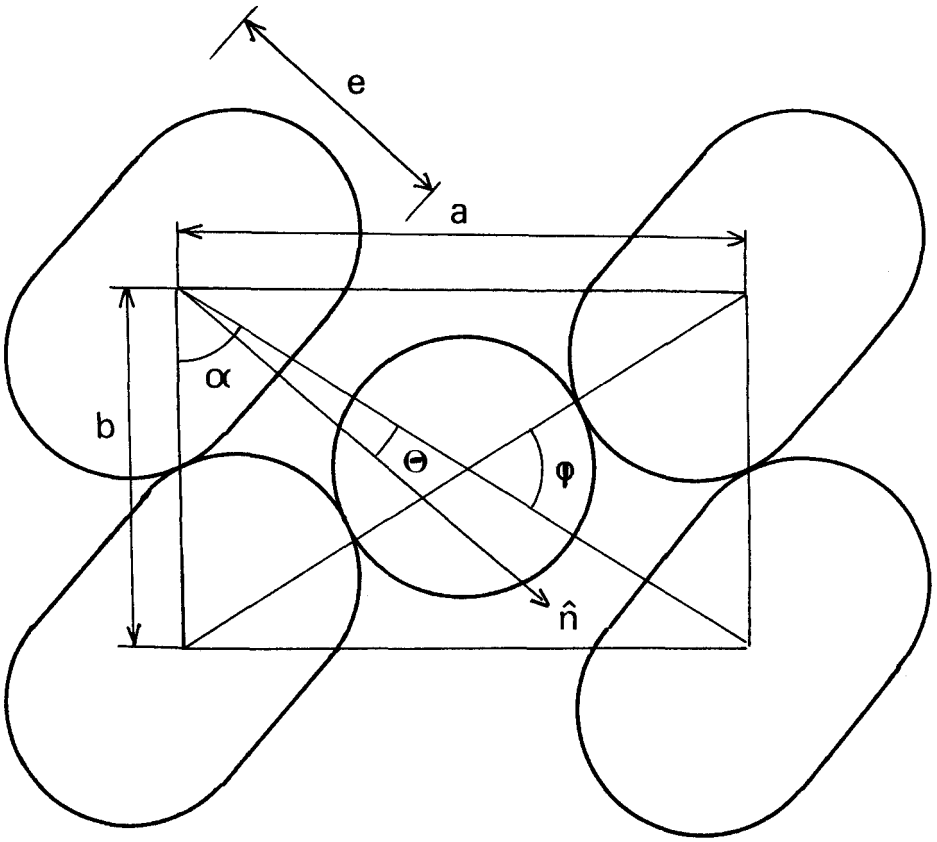

Figure 7 (*c*).

of the aromatic cores in the smectic E phases of the short alkyl chain compounds affects the electron density distribution along the layer normals and weakens the first Bragg harmonic of the smectic layers with respect to the second one, as indeed observed experimentally in the X-ray patterns of C-6-Br.

In a similar way as for the smectic E, the smectic B phases were characterized by the presence in the wide angle region of the X-ray patterns of only one rather sharp Bragg reflection around 4·4 Å, comparable to that generally observed with smectic B liquid crystals, as for instance with *N*-4′-*n*-alkoxybenzylidene-4-*n*-alkylanilines (*n*0·*m*) [16] or *p*,*n*-alkoxybenzylidene-*p*-chloroanilines [17]. This reflection is indicative of a two dimensional ordering of the molecules within the smectic layers and can easily be indexed as the d_{100} reflection from a two dimensional hexagonal lattice. The cell parameters are shown in table 4 and compared to similar cell parameters found in the literature for one other smectic B compound [17]. The molecular areas deduced from the cell parameters, $S=\sqrt{3}D^2/2\approx 22\,\text{Å}^2$ (see table 4), agree with what is normally expected for the lateral packing area of rod-like smectogenic molecules. The structure of the smectic B phase is closely related to that described for the smectic E phases; the only difference lies in the symmetry of the rectangular lattice whose cell parameters are $a=\sqrt{3}b=\sqrt{3}D$.

Finally, the smectic A phases were characterized by a single diffuse band in the wide angle region of the X-ray patterns, located at about 4·5 Å, indicative of the well-known liquid-like ordering of the molecules within the smectic layers.

Table 4. Wide angle Bragg reflections, d_{100}, and hexagonal lattice parameters of smectic B phases; D, length of unit cell side; S, molecular area.

Compound	d_{100}/Å	D/Å	S/Å^2
C-10-Cl	4·37	5·05	22·1
C-12-Cl	4·33	5·00	21·6
C-10-Br	4·42	5·10	22·5
C-12-Br	4·43	5·12	22·7
n-Cl [17]	4·3	4·96	21·4

5. Conclusion

In this work, a new series of pyridinium smectogens has been prepared and studied with differential scanning calorimetry, polarizing optical microscopy and X-ray diffraction. Their smectic structure was found to correspond to the stacking of single layers of upright molecules laterally arranged head to tail, with the anions sandwiched between the pyridinium rings. The same type of ordering had already been reported for other pyridinium smectic salts [3, 4]. However, deriving here advantage from the existence of ordered smectic E phases, with rich X-ray patterns, the lateral arrangement of the ionic end groups was described in detail. Segregated from the non-ionic moieties of the molecules, the ionic end groups were found to set in double layers with the oppositely charged species facing each other. Alternating with one another, the pyridinium rings and the anions are arranged in rows running along the two diagonals of the rectangular cell. It is of interest to point out that, owing to the presumably delocalized positive charge of the pyridinium rings, these pack themselves in a chevron-type structure, with their normal tending to point in the direction of the anions.

To conclude it is useful to make a final remark on the relation between the smectic structures observed and the amphiphilic character of the molecules. Molecules with three distinct constituent parts are expected to give rise to more complex segregation phenomena than usual smectogenic molecules with only two distinct parts. If occurring at all, the intramolecular segregation responsible for the smectic ordering may involve the formation of two or three types of periodically superposed sublayers, depending upon the degree of mutual incompatibility of the molecular moieties. In the present work, the electrical interactions overbalance the van der Waals effective repulsions, resulting in the formation of only two sublayers, one with the ionic parts of the molecules, the other with the non-ionic parts regardless of whether these are aromatic or aliphatic in nature.

6. Experimental

^{1}H NMR measurements were performed with a Bruker spectrometer (90 MHz WH90). Thermal stability was studied in the range from 30 to 180°C, at a scanning rate of 2·5°C/min, under nitrogen, with a Mettler thermogravimetric instrument (TC10A). Chlorine and iodine contents were determined by a potentiometric method.

6.1. *Preparation of the pyridinium bromides*

4-Hydroxy-4′-methoxybiphenyl (**I**) was synthesized by a classical method [18] using 4,4′-biphenyldiol (Aldrich) and dimethyl sulphate. Crystallization from ethanol gave white crystals (52·2 per cent yield): mp 181°C. Analysis calculated for $C_{13}H_{12}O_2$ (200·2):

C 77·97; H 6·04. Found: C 77·85; H 5·99. ^{1}H NMR (CD_3OD), $\delta = 2{\cdot}90$ (s, 1H, OH); 4·42 (s, 3H, OCH_3); 6·29, 6·43, 6·83, 6·97 (q, 8H, ArH).

ω-(4′-Methoxy-4-biphenylyloxy)alkyl bromide (**II**), α,ω-dibromoalkanes (Fluka) were used as received, except for α,ω-dibromododecane which was recrystallized from ethanol. 30 mmol of (**I**) were dissolved in 200 ml water containing 34·5 mmol NaOH. The mixture was stirred and heated up to 90°C until it became clear, 60 mmol of dibromoalkane, dissolved in 200 ml of hot CH_3OH, were added to the mixture, which was then heated under reflux for 65 hours. The solid reaction product was filtered out of the hot mixture and washed with hot CH_3OH. When dried, the crude solid was recrystallized from ethanol. Silica gel TLC (eluent CH_2Cl_2) and ^{1}H NMR showed that the solid product was a mixture of the expected brominated (**II**) derivative (72 per cent), $\delta = 3{\cdot}25$–$3{\cdot}35$ (t, 2H, $BrCH_2$), with appreciable amounts of methoxylated derivative (22·5 per cent), $\delta = 3{\cdot}28$ (s, 3H, CH_3OCH_2), 3·25–3·35 (t, CH_3OCH_2) and of hydroxylated derivative (5·5 per cent), $\delta = 3{\cdot}78$–$3{\cdot}35$ (t, 2H, CH_2OH). In TLC, the bromo derivative migrates first, followed by the methoxy and the hydroxy derivatives.

Although the crude product can be used without further purification in the quaternization reaction with pyridine, the separation of (**II**) from the mixture was performed either on silica columns (eluent: toluene/chloroform 50/15 v/v) or (for the bromododecyl derivative of low solubility) on silica gel PLC plates (Merck). $C_{19}H_{23}O_2Br$ (363·30), hexyl, 49·7 per cent yield (reaction: 50 hours), mp 121·1°C. Analysis calculated: C 62·8; H 6·38. Found: C 63·05; H 6·37. $C_{21}H_{27}0_2Br$ (391·35), octyl, 68·4 per cent yield (reaction: 70 hours), mp 118·0°C. Analysis calculated: C 64·50; H 6·96. Found: C 65·14; H 7·02. $C_{23}H_{31}O_2Br$ (419·40), decyl, 43·0 per cent yield (reaction: 43 hours), mp 117·4°C. Analysis calculated: C 65·87; H 7·45. Found: C 65·88; H 7·49. $C_{25}H_{35}O_2Br$ (447·96), dodecyl, 54·6 per cent yield (reaction: 55 hours), mp 116·3°C. Analysis calculated: C 67·10; H 7·88. Found: C 67·14; H 7·91.

2-[2-[2-(4′-methoxy-4-biphenylyloxy)ethoxy]ethoxy]ethyl bromide (**III**). This compound was prepared from 2-[2-[2-(4′-methoxy-4-biphenylyloxy)ethoxy]ethoxy] ethanol [19] using $SOBr_2$ in toluene in the presence of pyridine. It was recrystallized twice from methanol (35 per cent yield). $C_{19}H_{23}O_4Br$ (395·30). Analysis calculated: C 57·73; H 5·86. Found: C 57·63; H 5·84.

1-[ω-(4′-Methoxy-4-biphenylyloxy)alkyl]-pyridinium bromide (**IV**). A stirred solution of 2·2 mmol of (**II**) in 60 ml of dry pyridine (Riedel–de-Haen), freshly distilled over KOH, was heated at 50°C for 1 hour under nitrogen. The reaction mixture was kept at room temperature for 5 days. The solid crude product was filtered, washed with ether, and dissolved in methanol; the solution obtained was filtered and evaporated to dryness; finally, the solid was recrystallized from EtOH/EtAc and dried under vacuum at room temperature (98 per cent yield). $C_{24}H_{28}O_2NBr$, 1/2 H_2O (451·41), hexyl. Analysis calculated: C 63·85; H 6·47; N 3·10. Found: C 64·19; H 6·47; N 3·04. $C_{26}H_{32}O_2NBr$, 1/2 H_2O (479·46), octyl. Analysis calculated: C 65·13; H 6·93; N 2·92. Found: C 65·17; H 6·76; N 2·98. $C_{28}H_{36}O_2NBr$, 1/2 H_2O (507·52), decyl. Analysis calculated: C 66·26; H 7·34; N 2·75. Found: C 66·03; H 7·40; N 2·63. $C_{30}H_{40}O_2NBr$, 1/2 H_2O (535·57), dodecyl. Analysis calculated: C 67·28; H 7·71; N 2·62. Found: C 67·15; H 8·00; N 2·53.

^{1}H NMR ($CDCl_3$) for $C_{30}H_{40}O_2$ NBr, 1/2 H_2O (dodecyl): $\delta = 9{\cdot}433$–$9{\cdot}372$ (d, 2H, $2CHN^+$); 8·524–8·436–8·348 (t, 1H, $C\bar{H}CHCH$–Py^+); 8·117–8·048–7·967 (t, 2H, $CHC\bar{H}CH$–Py^+); 7·452–7·354, 7·927–6·826 (2d, 8H, Ar); 5·026–4·945–4·863 (t, 2H, CH_2N^+); 3·983–3·912–3·843 (t, 2H, CH_2O); 3·771 (s, 3H, CH_3O); 1·959–1·965, 1·199 (20H, 10 CH_2); 1·714 (s, bound H_2O). The same sample after 1 hour drying at 80°C

under vacuum: $\delta = 9{\cdot}481$–$9{\cdot}419$ (d, 2 H, CHN^+CH); 5·040–4·959–4·877 (t, 2 H, CH_2N^+); 1·714 (absent); other peaks without change. The same sample added with a drop of H_2O: $\delta = 9{\cdot}316$–$9{\cdot}254$ (d, 2 H 2CHN^+); 4·974–4·983–4·811 (t, 2 H, CH_2N^+); 4·632–4·612 (free H_2O); 1·773 (bound H_2O), other peaks without change.

The same quaternization procedure was applied to (**III**). $C_{24}H_{28}O_4NBr$, 1/2 H_2O (483·36). Analysis calculated: C 58·54; H 6·14; N 2·84. Found: C 58·45; H 6·05; N 2·71.

6.2. *Preparation of the other pyridinium salts*

6.2.1. *Chlorides* [7]

A solution of 1·33 mmol of (**IV**) in 100 ml of water/ethanol (80/20 v/v), with 6·65 mmol of AgCl, was heated in the dark for 5 days at 75°C, then a further 20 ml of ethanol was added. After filtration, the solution was evaporated to dryness, and the solid product recrystallized from methanol. $C_{26}H_{32}O_2NCL$, 1 H_2O (444·02), octyl. Analysis calculated: C 70·33; H 7·72; N 3·15; Cl 7·98. Found: C 69·66; H 7·73; N 2·93; Cl 8·00. $C_{28}H_{36}O_2NCl$, 1 H_2O (472·07), decyl. Analysis calculated: C 71·24; H 8·11; N 2·96; Cl 7·50. Found: C 69·97; H 7·98; N 2·82; Cl 7·58. $C_{30}H_{40}O_2NCl$, 1 H_2O (553·58), dodecyl. Analysis calculated: C 72·04; H 8·46; N 2·80; Cl 7·09. Found: C 71·01; H 8·34; N 2·65; Cl 7·00. ^1H NMR ($CDCl_3$). For $C_{30}H_{40}O_2NCl$, 1 H_2O, (dodecyl), $\delta = 9{\cdot}538$–$9{\cdot}479$ (d, 2 H, CHN^+CH); 8·564–8·476–8·403 (t, 1 H, $CHCHCH$–Py^+); 8·388–8·325–8·107 (t, 2 H, $CHCHCH$–Py^+); 5·067–4·987–4·912 (t, 2 H, CH_2N^+).

6.2.2. *Iodides* [8]

90 mmol of potassium iodide was added to a solution of 0·76 mmol of (**IV**) in 100 ml water/methanol (50/10 v/v. The mixture was stirred at 70°C for 48 hours. After cooling, the solid was filtered off, rinsed with water, dried, and recrystallized from methanol. $C_{30}H_{40}O_2NI$ (573·56), dodecyl. Analysis calculated: C 62·82; H 7·09; N 2·44; I 21·98. Found: C 62·94; H 7·00; N 2·37; I 21·40. ^1H NMR ($CDCl_3$). For $C_{30}H_{40}O_2NI$ (dodecyl); $\delta = 9{\cdot}306$–$9{\cdot}244$ (d, 2 H, CHN^+ CH); 8·570–8·482–8·397 (t, 1 H, $C\bar{H}CHCH$–Py^+); 8·143–8·071–7·987 (t, 2 H, $CHC\bar{H}CH$–Py^+); 4·948–4·870–4·785 (t, 2 H, CH_2N^+).

One of us (D.N.-R.) wishes to thank the Consejo Nacional de Ciencia y Technologia of Mexico and the Comité d'Etudes sur les Formations d'Ingénieurs for their financial support during this work.

References

[1] Gray, G. W., and Winsor, P. A. (editors), 1974, *Liquid Crystals and Plastic Crystals*, Vols. 1 and 2 (Wiley).
[2] Skoulios, A., and Luzzati, V., 1961, *Acta crystallogr.*, **14**, 278. Spegt, P., and Skoulios, A., 1964, *Acta crystallogr.*, **16**, 301. Abied, H., Guillon, D., Skoulios, A., Weber, P., Giroud-Godquin, A. M., and Marchon, J. C., 1987, *Liq. Crystals*, **2**, 269.
[3] Bazuin, C. G., Guillon, D., Skoulios, A., and Nicoud, J. F., 1986, *Liq. Crystals*, **1**, 181.
[4] Sudhölter, E. J. R., Engberts, J. B. F. N., and De Jeu, W. H., 1982, *J. phys. Chem.*, **86**, 1908.
[5] Skoulios, A., and Guillon, D., 1988, *Molec. Crystals liq. Crystals*, **165**, 317.
[6] Menschutkin, N., 1890, *Z. phys. Chem.*, **6**, 41.
[7] Cunningham, A. J., and Underwood, A. L., 1967, *Biochemistry*, **6**, 266.
[8] Knight, G. A., and Shaw, B. D., 1938, *J. chem. Soc.*, p. 682.
[9] Weast, R. C. (editor), 1975, *Handbook of Chemistry and Physics*, 56th edition (CRC Press).
[10] Belbeoch, B., Roulliay, M., and Tournarie, M., 1985, *C. r. hebd. Séanc. Acad. Sci., Paris*, **301-II**, 871.

[11] DOUCET, J., LEVELUT, A. M., LAMBERT, M., LIEBERT, L., and STRZELECKI, L., 1975, *J. Phys. Coll. Paris.*, **C1-36,** 13.
[12] DURAN, R., GUILLON, D., GRAMAIN, PH., and SKOULIOS, A., 1988, *J. Phys., Paris*, **49,** 1455.
[13] ISRAELACHVILI, J. N., 1985, *Intermolecular and Surface Forces* (Academic Press).
[14] WARD, D. L., RHINEBARGER, R. R., and POPOV, A. I., 1986, *Acta crystallogr.* C, **42,** 1771.
[15] KITAIGORODSKY, A. I., 1973, *Molecular Crystals and Molecules* (Academic Press).
[16] LEADBETTER, A. J., FROST, J. C., and MAZID, M. A., 1979, *J. Phys., Paris*, **40,** 325.
[17] SEURIN, P., GUILLON, D., and SKOULIOS, A., 1981, *Molec. Crystals liq. Crystals*, **71,** 51.
[18] APFEL, M. A., FINKELMANN, H., JANINI, G. M., LAUB, R. J., LUBMAN, B. H., PRICE, A., ROBERTS, W. L., SHAW, T. J., and SMITH, G. A., 1985, *Analyt. Chem.*, **57,** 851.
[19] DURAN, R., and GRAMAIN, PH., 1987, *Makromolek. Chem.*, **188,** 2001